BaV_3O_8: A possible Majumdar-Ghosh system with $S = \frac{1}{2}$

T. Chakrabarty,[1] A. V. Mahajan,[1,*] A. A. Gippius,[2,3] A. V. Tkachev,[2,3] N. Büttgen,[4] and W. Kraetschmer[4]

[1]*Department of Physics, IIT Bombay, Powai, Mumbai 400076, India*

[2]*Faculty of Physics, Moscow State University, Moscow 119991, Russia*

[3]*A. V. Shubnikov Institute of Crystallography, Moscow 119333, Russia*

[4]*Institute of Physics, University of Augsburg, D-86135 Augsburg, Germany*

(Received 1 April 2013; revised manuscript received 5 June 2013; published 31 July 2013)

BaV_3O_8 contains magnetic $V^{4+}(S = 1/2)$ ions and also nonmagnetic $V^{5+}(S = 0)$ ions. The V^{4+} ions are arranged in a coupled Majumdar-Ghosh chainlike network. A Curie-Weiss fit of our magnetic susceptibility $\chi(T)$ data in the temperature region of 80–300 K yields a Curie constant $C = 0.39$ cm^{3}K/mole V^{4+} and an antiferromagnetic Weiss temperature $\theta = -26$ K. The χ(T) curve shows a broad maximum at $T \simeq 25$ K indicative of short-range order (SRO) and an anomaly corresponding to long-range order (LRO) at $T_N \sim 6$ K. The value of the "frustration parameter" ($f = |\theta/T_N| \sim 5$) suggests that the system is moderately frustrated. Above the LRO temperature, the experimental magnetic susceptibility data match well with the coupled Majumdar-Ghosh (or $J_{nn} - J_{nnn}$ Heisenberg) chain model with the ratio of the nnn (next-nearest neighbor) to nn (nearest neighbor) magnetic coupling $\alpha = 2$ and $J_{nnn}/k_B = 40$ K. In a mean-field approach when considering the interchain interactions, we obtain the total interchain coupling to be about 16 K. The LRO anomaly at T_N is also observed in the specific heat $C_P(T)$ data and is not sensitive to an applied magnetic field up to 90 kOe. A ^{51}V NMR signal corresponding to the nonmagnetic vanadium was observed. Anomalies at 6 K were observed in the variation with temperature of the ^{51}V NMR linewidth and the spin-lattice relaxation rate $1/T_1$ indicating that they are sensitive to the LRO onset and fluctuations at the magnetic V sites. The existence of two components (one short and another long) is observed in the spin-spin relaxation rate $1/T_2$ data in the vicinity of T_N. The shorter component seems to be intimately connected with the magnetically ordered state. We suggest that both magnetically ordered and nonlong-range-ordered (non-LRO) regions coexist in this compound below the long-range-ordering temperature.

DOI: 10.1103/PhysRevB.88.014433 PACS number(s): 75.10.Pq, 75.40.Cx, 76.60.−k

I. INTRODUCTION

The field of low-dimensional and geometrically frustrated magnetism is an active area of research in solid state physics.[1–3] In the last few decades, special emphasis has been laid on low-dimensional spin systems[4,5] such as chains, square lattices, ladders, especially after the discovery of high-temperature superconductivity in cuprates.[6] In the case of one-dimensional (1D) antiferromagnetic (AF) chains, the scenario becomes even more interesting if in addition to a nearest-neighbor (nn) interaction, a frustrating next-nearest-neighbor (nnn) interaction is also present. Depending on the ratio of the nnn to nn coupling (J_{nnn}/J_{nn}) in these so-called "Majumdar-Ghosh" (MG) chains (or $J_{nn} - J_{nnn}$ Heisenberg),[7] distinct magnetic phases are formed. For $J_{nnn}/J_{nn} \geqslant 0.24$, the ground state is spontaneously dimerized with an energy gap in the excitation spectrum.[8]

A number of Cu-based ($3d^9$) AF systems that can be described by the MG (or $J_{nn} - J_{nnn}$ Heisenberg) chain model have been investigated in the past. Some examples are $CuCrO_4$,[9] $(N_2H_5)CuCl_3$,[10] and $Cu(ampy)Br_2$.[11] Of these, $CuCrO_4$ is thought to be close to the MG point ($J_{nnn}/J_{nn} \simeq 0.5$)[9] and $(N_2H_5)CuCl_3$ is close to the quantum critical point ($J_{nnn}/J_{nn} = 0.24$).[10] Surprisingly, it appears that the few vanadium-based ($3d^1$) $S = 1/2$ low-dimensional AF systems that have been investigated have exclusively been either of the dimer type [CsV_2O_5 (Ref. 12)], 1D uniform chain type [NaV_2O_5 (Ref. 13)] or ladder type [$(VO)_2P_2O_7$ (Ref. 14), CaV_2O_5 (Ref. 15)]. On the other hand, we were unable to find in literature any examples of vanadium-based ($3d^1$) $S = 1/2$ systems described by the $J_{nn} - J_{nnn}$ Heisenberg chain model. We have been exploring low-dimensional oxides with the intention of unraveling novel magnetic properties. It seems interesting to investigate systems where the magnetic exchanges arise from the overlap of the (say) d_{xy} orbitals (via the oxygen p) rather than the $d_{x^2-y^2}$ orbitals as in the Cu-based systems. In this paper, we report our studies on the yet unexplored system BaV_3O_8 via magnetization, heat capacity and ^{51}V nuclear magnetic resonance (NMR) measurements. The susceptibility $\chi(T)$ data exhibit a broad maximum at 25 K signifying short-range order (SRO). The appearance of long-range order (LRO) at $T_N \sim 6$ K is evidenced in the susceptibility as well as the heat capacity data. From our $\chi(T)$ data, we infer that the linkages between the magnetic ($S = 1/2$) V^{4+} ions in this compound are like those of an MG chain with $\alpha \approx 2$. The NMR signal from the magnetic ^{51}V ions could not be observed most probably due to the strong on-site fluctuations of the V^{4+} moment giving rise to a wipeout of the NMR signal. On the other hand, a ^{51}V NMR signal corresponding to the nonmagnetic V^{5+} nuclei was easily observed. Further, the evolution of its line shape, spin-lattice relaxation rate $1/T_1$, and spin-spin relaxation rate $1/T_2$ clearly indicates that they are sensitive to the LRO onset and are driven by the fluctuations of the magnetic V^{4+} ions. In the vicinity of LRO, the existence of two components is observed in the spin-spin relaxation data indicating the co-existence of non-LRO and magnetically ordered regions.

II. SAMPLE PREPARATION, CRYSTAL STRUCTURE, AND EXPERIMENTAL DETAILS

BaV_3O_8 is a monoclinic system (space group $P2_1/m$)[16] containing both magnetic and nonmagnetic vanadium ions.

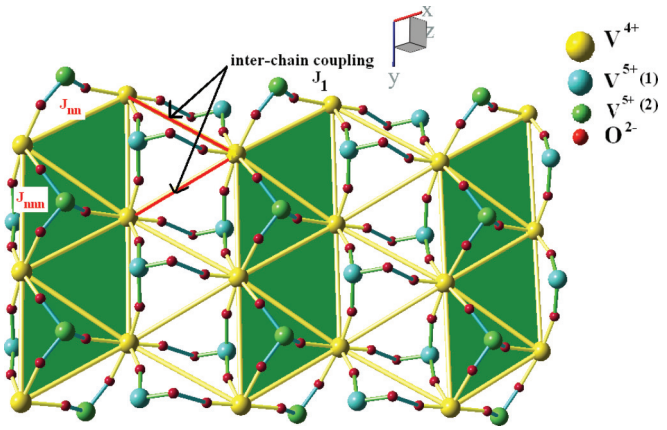

FIG. 1. (Color online) Schematic diagram of the coupled-MG chain network formed by the V^{4+} ions. Possible interaction paths between the V^{4+} ions are shown in the figure.

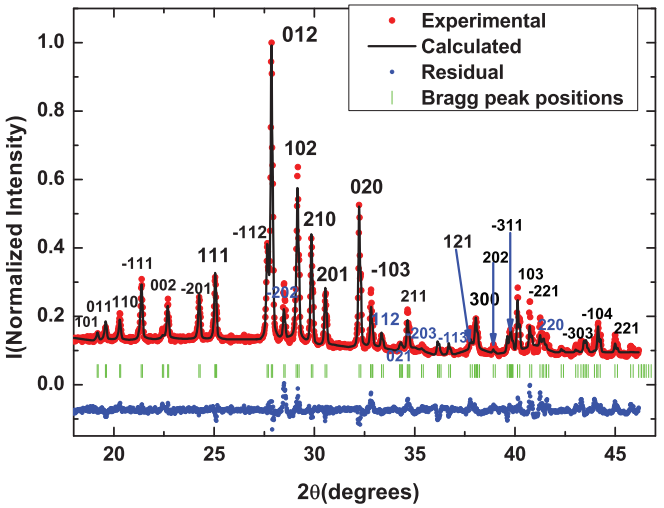

FIG. 2. (Color online) The x-ray diffraction pattern of BaV_3O_8 is shown along with its Bragg peak positions. The red points are the experimental data, the black curve is the FULLPROF generated refinement pattern, the green markers are the Bragg peak positions, and the blue points represent the difference between the measured and the calculated intensities.

Among the three vanadium ions in the unit cell, two are in the V^{5+}($S = 0$, nonmagnetic) state and one is in the V^{4+} ($S = 1/2$) state. The V^{4+} ions appear to form chains where the interactions between the magnetic vanadium ions are likely mediated through oxygen (O^{2-}) and the nonmagnetic V^{5+} ions (see Fig. 1). Based on the structure, one expects comparable nn and nnn interactions within the chain. The interchain interactions are expected to be weaker. One might, therefore, think of this system as made of coupled MG chains. Since no magnetic data have been reported on BaV_3O_8 as yet, we have pursued the problem further and report here the preparation, magnetic susceptibility $\chi(T)$, heat capacity $C_P(T)$, and ^{51}V NMR measurements on BaV_3O_8.

BaV_3O_8 was prepared by standard solid state reaction methods. In the first step we prepared BaV_2O_6 by firing stoichiometric amounts of $BaCO_3$ (Alfa Aesar-99.95%) and V_2O_5 (Aldrich-99.6%) at 680 °C for 28 hours. In the next step, we fired BaV_2O_6 and VO_2 (Alfa Aesar-99.5%) at 700 °C for 36 hours in a sealed quartz tube. X-ray diffraction (xrd) patterns were collected with a PANalytical x-ray diffractometer using Cu K_α radiation ($\lambda = 1.541\,82$ Å). The Rietveld refinement of the xrd data was carried out using the FULLPROF software[17](see Fig. 2). Whereas the refinement was attempted using two different monoclinic space groups [$P2_1/m$ (Ref. 16) and$P2_1$ (Ref. 18)], we obtained better results using the first one. The refined atomic coordinates are given in Table I.

The cell parameters obtained for BaV_3O_8 (Space group: $P2_1/m$, $a = 7.432$ Å, $b = 5.549$ Å, $c = 8.200$ Å, $\beta = 107.207°$) are in agreement with those of Ref. 16. The goodness of the Rietveld refinement as defined by the following parameters is $R_p = 18.6\%$, $R_{wp} = 14\%$, $R_{exp} = 11.10\%$, and $\chi^2 = 1.58$. By simple valence counting, from among the three vanadium ions in the unit cell, two would be in the V^{5+} ($S = 0$, nonmagnetic) state and one in the V^{4+} ($S = 1/2$) state. In the unit cell of BaV_3O_8, V^{5+} ions form tetrahedra with the oxygen ions whereas the V^{4+} ions form pyramids with the oxygen ions.

The various bond angles and bond lengths are given in Tables II and III. The possible interaction paths between the V^{4+} ions are illustrated in Fig. 1. The V^{4+} ions appear to be arranged in a coupled MG chainlike fashion (along the crystallographic b-direction) and further form corrugated planes as shown in Fig. 1. If we concentrate on an MG chain it can be seen that the V^{4+} ions form triangular plaquettes and in a given triangular plaquette the bond distances and the bond angles between any two vanadiums are nearly the same. This suggests a frustrated scenario of an MG chain with comparable J_{nnn} and J_{nn}. The coupling between the V^{4+} ions of adjacent chains (J_1) (in a corrugated plane) might be weaker than the intrachain V^{4+}- V^{4+} interaction since the interchain V^{4+}- V^{4+} interaction path consists of one extra oxygen ion. There could also be a weaker V^{4+}- V^{4+} interaction (J_2) in a direction perpendicular to the corrugated plane of the coupled-MG chains. Therefore, based on the structural details alone, one might expect SRO in this system.

The temperature dependence of the magnetization M was measured in a magnetic field of 5 kOe in the temperature T range 2–300 K using a vibrating sample magnetometer (VSM) attached to a Quantum Design physical property measurement system (PPMS). The temperature dependence of the specific heat has been measured in the temperature range of 2–270 K by

TABLE I. Atomic positions in BaV_3O_8.

Atoms	Coordinates x (Å)	y (Å)	z(Å)	Occupancy
Ba(2e)	0.212	0.250	−0.099	1.00
V^{5+}(2e)	0.072	0.250	0.361	1.00
V^{4+}(2e)	0.294	0.750	0.216	1.00
V^{5+}(2e)	0.585	0.250	0.316	1.00
O1(4a)	0.480	0.494	0.200	1.00
O2(2e)	0.432	0.750	0.476	1.00
O3(4a)	0.156	0.505	0.261	1.00
O4(2e)	0.167	0.750	0.019	1.00
O5(2e)	−0.171	0.250	0.319	1.00
O6(2e)	−0.145	0.250	0.545	1.00

TABLE II. Bond angles between various vanadium and oxygen ions in BaV_3O_8.

Angles	Description	Value
V^{4+}-O^{2-}(1)-V^{5+}(2)	intrachain	137.07°
O^{2-}(1)-V^{5+}(2)-O^{2-}(2)	intrachain	113.08°
V^{5+}(2)-O^{2-}(2)-V^{4+}	intrachain	147.75°
V^{4+}-O^{2-}(3)-V^{5+}(1)	intrachain	163.76°
O^{2-}(3)-V^{5+}(1)-O^{2-}(3)	intrachain	101.01°
O^{2-}(1)-V^{5+}(2)-O^{2-}(1)	intrachain	104.89°
O^{2-}(3)-V^{5+}(1)-O^{2-}(5)	interchain	112.44°
V^{5+}-(1)O^{2-}(5)-O^{2-}(4)	interchain	83.15°
O^{2-}(5)-O^{2-}(4)-V^{4+}	interchain	145.43°

using a Quantum Design PPMS. The field-sweep NMR spectra were recorded by means of a home-built phase coherent pulsed spectrometer by sweeping the magnetic field at several fixed frequencies. Typical pulse lengths were 5 and 10 ms for the $\pi/2$ and π pulses, respectively, with a pulse separation of 50 μs. At each temperature, the area under the spin-echo magnitude was integrated in the time domain and averaged over mutiple scans. The ^{51}V nuclear spin-lattice relaxation was measured by the inversion recovery method using a $\pi - t - \pi/2 - \tau - \pi$ pulse sequence with $\tau = 50$ μs and variable t. To obtain the saturation magnetization M_0, the first π pulse was switched off every even scan. Subtracting results of odd and even scans one obtains M_t, which is generally fit to $M_t = -M_0 + 2M_0 e^{(-t/T_1)}$. In the present case, two components were found in the relaxation behavior. Consequently, the above equation was modified to accommodate two exponentials with different coefficients. The spin-spin relaxation rate $1/T_2$ measurements were performed in the temperature range of 1.65–9.2 K at a fixed frequency of 70 MHz on the maximum of the spectra (at an applied field 62.6 kOe). The decay of the spin echo (integrated intensity) following a $\pi/2$ -π pulse sequence was monitored as a function the pulse separation τ.

III. RESULTS

With decreasing temperature, χ follows the Curie-Weiss law and shows a broad maximum at about 25 K (see Fig. 3). With a further decrease in T, a sharp drop is observed in $\chi(T)$ at $T_N \simeq 6$ K. A Curie-like upturn is observed at lower

TABLE III. The bond lengths of the various vanadium-oxygen linkages in BaV_3O_8.

Bonds	Description	Value
V^{4+}-O^{2-}(1)	intrachain	2.01 Å
O^{2-}(1)-V^{5+}(2)	intrachain	1.71 Å
V^{5+}(2)-O^{2-}(2)	intrachain	1.74 Å
O^{2-}(2)-V^{4+}	intrachain	2.07 Å
V^{4+}-O^{2-}(3)	intrachain	1.81 Å
O^{2-}(3)-V^{5+}(1)	intrachain	1.83 Å
V^{5+}(1)-O^{2-}(5)	interchain	1.74 Å
O^{2-}(5)-O^{2-}(4)	interchain	2.78 Å
O^{2-}(4)-V^{4+}	interchain	1.62 Å

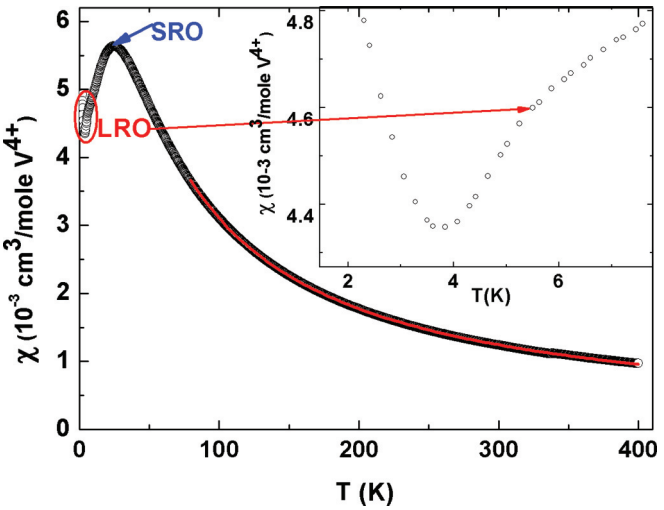

FIG. 3. (Color online) The temperature dependence of the susceptibility $\chi = M/H$ at $H = 5$ kOe. LRO, and SRO regions are indicated. The inset shows a zoom of the low-T region where the LRO region is marked. The red line shows the Curie-Weiss fit in the temperature range of 80–300 K.

temperatures. From the Curie-Weiss fit $\chi(T) = \chi_0 + C/(T - \theta_{CW})$ in the range 80–300 K, we get the T-independent susceptibility $\chi_0 = 5.07 \times 10^{-5}$cm^3/mole V^{4+}, the Curie constant $C = 0.39$ cm^{3}K/mole V^{4+}, and the Curie-Weiss temperature $\theta_{CW} = -26$ K. With $S = 1/2$ for the V^{4+} ion, this Curie constant yields a g factor of 2.04 indicating a very small spin-orbit coupling. From $\chi_0 = 5.07 \times 10^{-5}$ cm^3/mole V^{4+}, we obtain the Van Vleck susceptibility $\chi_{VV} = \chi_0 - \chi_{core} = 1.94 \times 10^{-4}$ cm^3/mole V^{4+} where χ_{core}, is the core diamagnetic susceptibility equal to -1.43×10^{-4} cm^3/mole formula unit.[19] The broad maximum at 25 K might signify the onset of SRO in the MG chains. The second anomaly observed at T_N (see inset of Fig. 3) perhaps evidences the onset of LRO. With the frustration parameter $f = \frac{|\theta_{CW}|}{T_N} \sim 5$ it appears that the system is moderately frustrated.[20]

The magnetic susceptibility of BaV_3O_8 was modeled using the exact diagonalization results for the susceptibility $\chi_{MG}(g, \alpha, J_{nn})$ of a single chain provided by Heidrich-Meissner *et al.*[21,22] (where $\alpha = J_{nnn}/J_{nn}$). Since our experimental results did not match those of the isolated Majumdar-Ghosh chain simulation for different parameters α and J_{nn}, we used the expression for a coupled Majumdar-Ghosh chain model, where the interchain spin exchange is treated within a mean-field approach,[23] as Eq. (1):

$$\chi_{\text{coupled MG}}(T) = [\chi_{MG}/(1 - \lambda\chi_{MG})] + \chi_0. \quad (1)$$

Here, λ is the mean-field parameter

$$\lambda = (z_1 J_1 + z_2 J_2)/N_A g^2 \mu_B^2, \quad (2)$$

where J_1 and J_2 are the interchain coupling constants within the plane and perpendicular to the plane, respectively, as shown schematically in Figs. 1 and 4. The corresponding number of neighbours is z_1 and z_2. We found the best agreement of our data with the coupled MG chain model calculations for $\alpha = 2$, $J_{nnn}/k_B = 40$ K, and $\lambda = 21$ mol/cm^3 (cf. red solid line in Fig. 5). Taking $z_1 = z_2 = 2$ (see Figs. 1 and 4),

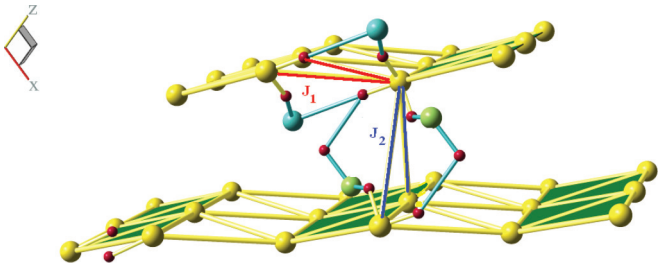

FIG. 4. (Color online) Possible interchain interaction paths between the V^{4+} ions.

we get $J_1 + J_2 = 16$ K. We remark in passing that the MG point itself is exemplified by $\alpha = 0.5$. The positive sign of the net interchain coupling constant indicates a ferromagnetic interaction. The significant interchain interactions seem to drive the system to a LRO state at low temperature. Whereas fitting of our bulk susceptibility data are indeed suggestive of a coupled MG chain scenario, we caution that any definitive conclusions need to be backed up by additional work such as neutron scattering measurements, density functional theory calculations to estimate the relative exchange couplings.

The heat capacity data of BaV_3O_8 are shown in Fig. 6 and exhibit a sharp anomaly at about 5.8 K. This is close to the transition temperature T_N measured in $\chi(T)$. The transition temperature does not shift with H up to 90 kOe. We have modeled the lattice contribution using the Debye model in the T-range 60–110 K. The measured heat capacity could be fit with a combination of two Debye functions of the type given below with coefficients C_1 and C_2 (see Fig. 6),

$$C_p = 9Nk_Bn(T/\theta_D)^3 \int_0^{\theta_D/T} [x^4e^x/(e^x-1)^2]dx, \qquad (3)$$

where n is the number of atoms in a formula unit, N is the Avogadro number, k_B is the Boltzmann constant, and θ_D is the relevant Debye temperature. The fit yields Debye temperatures

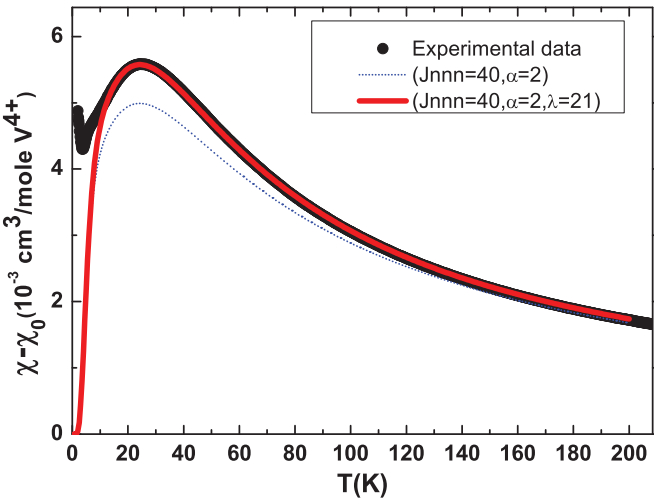

FIG. 5. (Color online) The temperature dependence of $\chi - \chi_0$ at $H = 5$ kOe (open circles). The red and the blue dotted (from top to bottom) lines represent the exact diagonalization results of Refs. 21 and 22 with interchain interaction ($\alpha = 2$, $\lambda = 21$) and without interchain interaction ($\alpha = 2$, $\lambda = 0$), respectively.

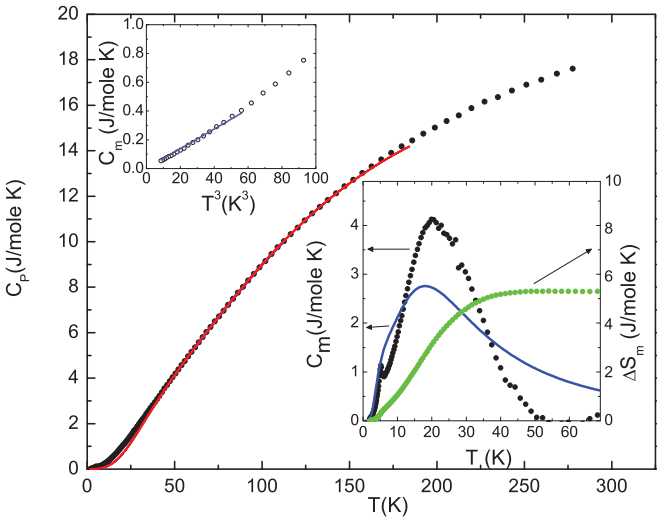

FIG. 6. (Color online) The temperature dependence of specific heat of BaV_3O_8; the inset on the right displays the magnetic contribution to the heat capacity (black filled circles). The red line represents the lattice heat capacity (see text). The blue line in the lower inset represents the exact diagonalization results of Refs. 21 and 22 (with $\alpha = 2$, $\lambda = 0$). Note that the total heat capacity of the main figure is normalized to the number of atoms (12 per formula unit) whereas the magnetic heat capacity in the inset is normalized to the number of magnetic atoms, i.e., one for each formula unit. The green data points (right axis) show the change of entropy with T. The upper inset shows the linear temperature dependence of the magnetic specific heat with T^3. The solid line is a linear fit to low-temperature data.

of 180 and 580 K and their coefficients 0.25 and 0.52, respectively. Upon subtracting the lattice heat capacity with the above parameters, we obtain the magnetic contribution to the heat capacity $C_m(T)$.

Subsequently, the entropy change (ΔS) was calculated by integrating the C_m/T data (see Fig. 6, right inset). The entropy change from about 50 to 2 K is about 5.4 J/K, which is more than 90% of the value for a $S = 1/2$ system [$R \ln(2S + 1)$]. The small disparity may be associated with the uncertainty in extracting the lattice contribution. Note also that, upon cooling, most of the entropy decrease has already taken place above T_N. This is a fingerprint of strong intrachain interactions in the system which give rise to SRO. The heat capacity of a model MG chain corresponding to $\alpha = 2$ and $J_{nnn}/k_B = 40$ K is shown in the Fig. 6 (right inset) by a blue solid line. The experimental magnetic heat capacity is similar in magnitude to the calculated curve. The small difference seen here can easily arise from uncertainties associated with the estimation of the lattice heat capacity. We observed a linear dependence of magnetic heat capacity with T^3 below 4 K (see Fig. 6, left inset) which suggests the presence of antiferromagnetic magnons in the ordered state.[24]

We were unable to detect the NMR signal associated with the magnetic V^{4+} nuclei of BaV_3O_8. This is because of a strong on-site local moment, which naturally couples well with its own nucleus. The fluctuations of this moment are very effective in causing a fast relaxation of the nuclear magnetization. This makes the detection of its NMR signal difficult. In Cs_2CuCl_4 as

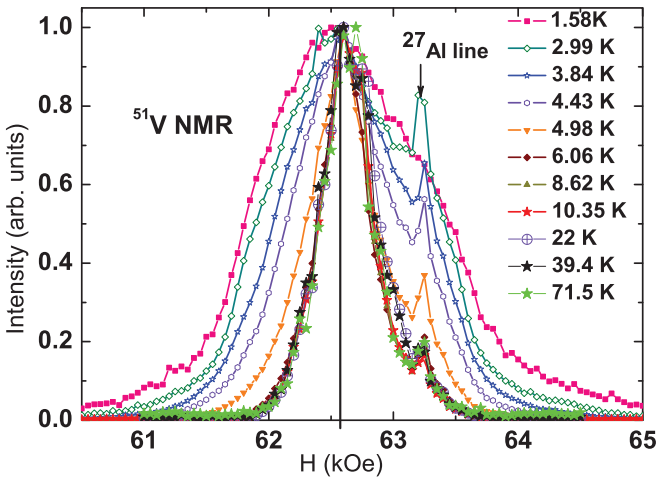

FIG. 7. (Color online) The ^{51}V spectra of BaV_3O_8 at different temperatures obtained by sweeping the field (the ^{27}Al signal is extrinsic and originates from the probehead) at a frequency of 70 MHz.

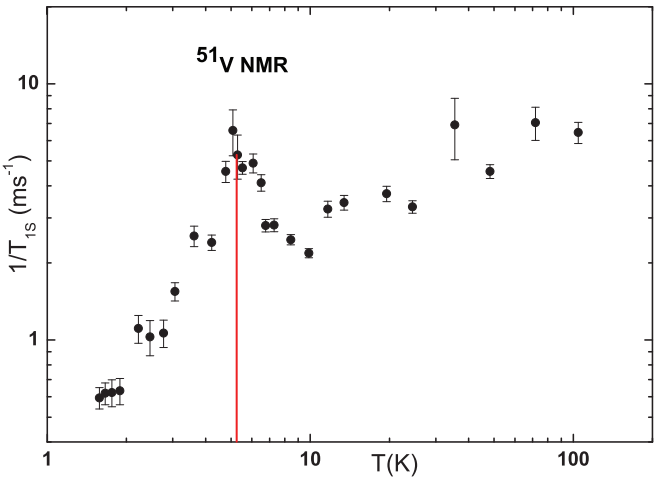

FIG. 9. (Color online) The temperature dependence of the spin-lattice relaxation rate ($1/T_1$) corresponding to the faster component. The red vertical line marks T_N.

well, an NMR signal from the ^{63,65}Cu nuclei was not detected probably for similar reasons.[25] On the other hand, the NMR signal from the nonmagnetic V^{5+} nuclei in BaV_3O_8 was easily observed. The spectrum is rather broad at 71.5 K with the full width at half maximum FWHM of about 0.43 kOe and the total extent of the spectrum of about 1.6 kOe (see Fig. 7). The FWHM increases slightly with decreasing temperature down to about 6K and increases drastically below that (see Fig. 8), which must be associated with the onset of LRO already indicated in $\chi(T)$ and $C_P(T)$ data. This implies that the V^{5+} nuclei are sensitive to the internal magnetic field arising in this compound. It is shown in Fig. 8 that FWHM in LRO phase ($T = 1.85$ K) decreases with H although it tends to the value

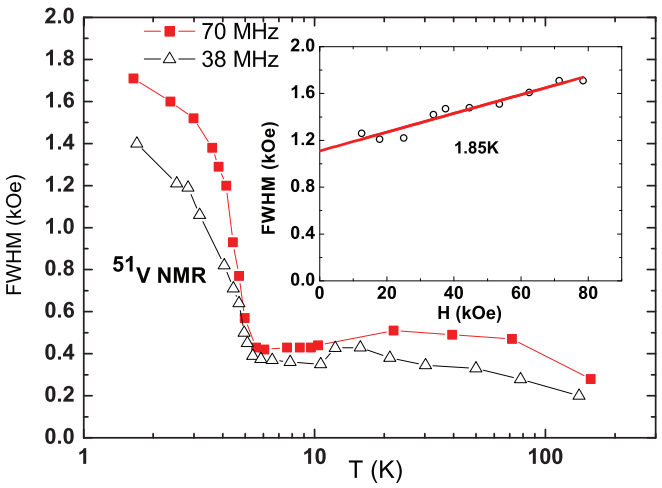

FIG. 8. (Color online) Temperature dependence of FWHM measured at fixed frequencies of 38 MHz (black open triangles) and 70 MHz (red closed squares) for BaV_3O_8. The pulse separation is 50 μs between the pulses of the spin-echo sequence irradiating ^{51}V nuclei. The inset shows the small variation in FWHM with the change in magnetic field measured at 1.85 K. The red line is a linear fit indicating the slight decrease in FWHM with decrease in magnetic field.

of about 1.1 kOe in zero field, which is 2–3 times more than the FWHM above T_N. Thus the externally applied magnetic field H is not the only source of such a broadening, however, the ^{51}V NMR shift does not change much with temperature, which indicates that the V^{5+} ions are very weakly coupled with the electrons of the magnetic vanadium (V^{4+}) ions.

We have measured the recovery of the longitudinal ^{51}V nuclear magnetization as a function of temperature to probe the low-energy spin excitations. The resulting recovery could be fitted well with a double exponential (consisting of a short and a long component) at all temperatures. The recovery was found to follow

$$1 - M(t)/M_o = B_s e^{(-t/T_{1S})} + B_L e^{(-t/T_{1L})} + C_1. \quad (4)$$

Here, T_{1S} and T_{1L} represent the short and the long components of T_1, B_S and B_L stand for their relative weights, respectively, and C_1 is a constant.[26] As seen in the structure, two inequivalent V^{5+} ions are present in BaV_3O_8 (see Fig. 1). One of them [$V^{5+}(2)$] is near the center of a triangular plaquette and appears coupled to three V^{4+} ions. The other vanadium [$V^{5+}(1)$] seems coupled to two V^{4+} ions via oxygen. Whereas it is not clear as to the relative magnitudes of the associated transferred hyperfine couplings in the above two cases, the relevant bond angles and bond lengths suggest that the various V^{4+}-O-V^{5+} couplings may not be too much different from each other. Therefore the $V^{5+}(2)$, which is hyperfine coupled to three V^{4+} might be expected to have a shorter T_1 compared to that for $V^{5+}(1)$. The variation of the faster rate $1/T_{1S}$ with temperature is shown in Fig. 9 (the slower component has the same qualitative behavior). As seen from this figure, a distinct anomaly of $1/T_1$ is observed at T_N.

Additionally, we measured the temperature dependence of the transverse decay and obtained the spin-spin relaxation rates $1/T_2$ presented in Fig. 10. As seen from the raw data at 2.22 K in Fig. 10 (right inset), the decay has two components shown by the two dashed lines. Consequently, we have fit the data at

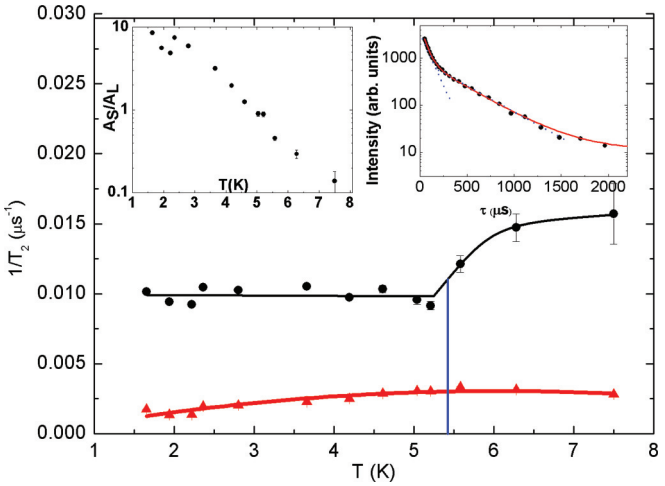

FIG. 10. (Color online) The variation of the ^{51}V spin-spin relaxation rates $1/T_{2S}$ and $1/T_{2L}$ with temperature is shown. The solid lines are drawn as guides to the eye. The blue vertical line points to the LRO temperature. The left inset shows the variation of the relative weight of the fast to slow component of T_2 with temperature. The right inset shows the spin-spin relaxation curve at 2.22 K. Here, the black circles correspond to experimental data and the red curve is a double exponential fit. The blue dashed lines correspond to the fast relaxing and slow relaxing components.

each temperature to a double exponential function

$$M_t = A_s e^{(-2\tau/T_{2S})} + A_L e^{(-2\tau/T_{2L})} + C_2. \quad (5)$$

Here, T_{2S} and T_{2L} denote the shorter and the longer components, respectively, A_S and A_L stand for their relative weights, respectively, and C_2 is a constant. The variation of $1/T_{2S}$ and $1/T_{2L}$ with temperature is shown in Fig. 10. As seen from Fig. 10, the short component, $1/T_{2S}$, exhibits a pronounced ∼50% decrease in the vicinity of T_N, while the longer one, $1/T_{2L}$, is insensitive to the magnetic ordering. The relative weight of the faster component (A_S/A_L) decreases monotonically with increasing temperature (as seen in the inset of Fig. 10) varying from about 10 at 1.5 K to about 0.1 at about 7.5 K. As is evident, at higher temperatures the spin-spin relaxation is dominated by the longer component. There is, therefore, a larger uncertainty in T_{2S} at higher temperatures. We also note that there is no sharp anomaly in the temperature dependence of A_S/A_L near T_N. Finally, it seems natural to think that A_S/A_L represents the relative amount of magnetically ordered regions with respect to non-LRO regions.

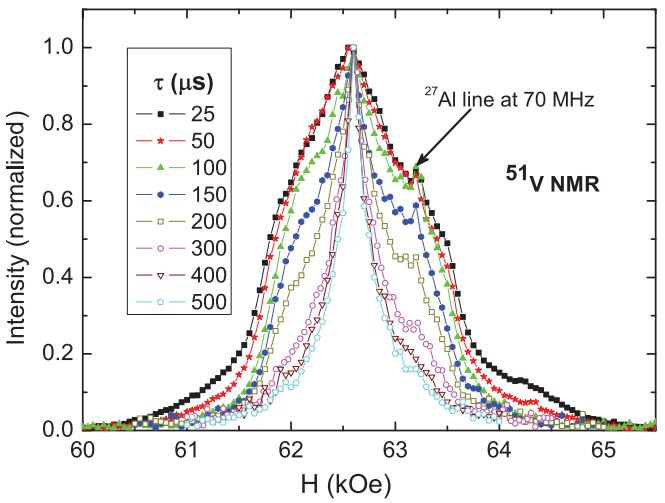

FIG. 11. (Color online) The variation of ^{51}V NMR spectra (ν = 70 MHz and T = 2.35 K) with the separation of pulses τ.

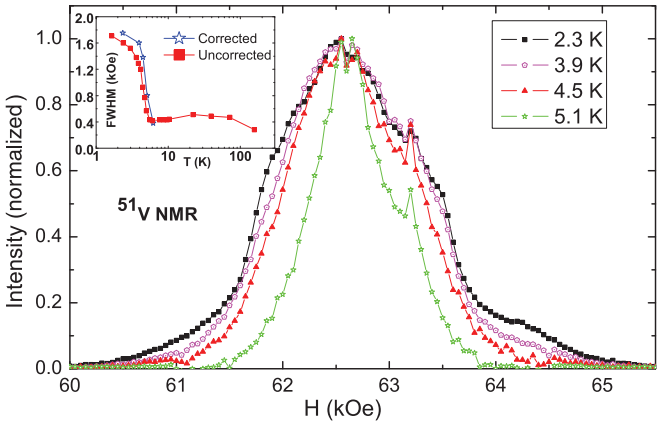

FIG. 12. (Color online) The corrected ^{51}V NMR spectra containing only the short T_2 component are shown at different temperatures (see text for details). Linewidth vs temperature plot for these spectra are shown in the inset where the filled symbols represent uncorrected data while the open symbols are identical data from Fig. 8 at 70 MHz.

Given the above information, it is clear that the ^{51}V NMR line shape in the low-temperature regime is affected by the measurement conditions, in particular, by the pulse separation τ between the $\pi/2$ and the π pulse. This is clearly seen in Fig. 11 where the ^{51}V spectra powder pattern is displayed at fixed frequency and temperature, but for different pulse separations τ. A broader resonance line is observed for smaller τ. This might be the reason for the observation of Fig. 8 where the FWHM keeps increasing with decreasing temperature without saturation even well below T_N. It is also worth noting that even above T_N, where no ordered moments are expected, a contribution to the width from the shorter T_2 remains. We have attempted to obtain the contribution to the line shape only from the faster T_{2S} component (i.e., the one originated from the magnetic regions) in the following manner. With a large pulse separation like $\tau = 500$ μs, the line shape contains the contribution only from the slow component. This is corrected using T_{2L} and the spectrum from only the long component is obtained at $\tau = 0$. Then with our shortest pulse separation $\tau = 25$ μs, the spectrum was measured. This contains both the fast and the slow components with dominating fast component at low temperatures. This is corrected for T_{2S} and the spectrum at $\tau = 0$ is obtained. We then subtract the first data set (T_{2L} dominated) from the latter. The resulting spectrum contains the contribution of only the faster T_2 component (one can see though that in the temperature region where $A_S/A_L \sim< 1$, this method suffers from a large uncertainty). The resulting spectra at various temperatures are shown in Fig. 12. The inset shows the linewidth obtained from such spectra which arises only from the magnetic regions. It is higher than the uncorrected data and also has a sharper variation near T_N.

IV. CONCLUSION

In this work, we have reported the crystal structure, magnetization, heat capacity, and NMR measurements on a new vanadium-based magnetic system BaV_3O_8. According to the crystallographic symmetry, the arrangement of the magnetic ions in BaV_3O_8 is like that of a coupled Majumdar-Ghosh chain with the possibility of three dimensional interactions. We found that the magnetic susceptibility shows a broad maximum at about 25 K indicating magnetic short-range order followed by a sharp anomaly at $T_N = 6$ K due to long-range order. The value of the 'frustration parameter' ($f = |\theta|/|T_N| \sim 5$) suggests that the system is moderately frustrated. Our susceptibility data above 15 K are well described by the coupled Majumdar-Ghosh chain model with the ratio of the nnn to nn magnetic coupling $\alpha = 2$ and $J_{nnn}/k_B = 40$ K. Considering the interchain interactions in the mean-field approach, we obtain the total interchain coupling $J_{nn}/k_B = 16$ K. However, a validation of the above conclusions would need input from techniques such as inelastic neutron scattering, density functional theory calculations, etc. From the magnetic contribution of the heat capacity C_m we find that upon cooling, most of the entropy decrease has already taken place at temperatures above T_N. This attests to the strong intrachain interactions in the system, which give rise to SRO. Below the LRO temperature of 6 K, the magnetic heat capacity follows well a T^3 behavior suggesting antiferromagnetic magnon excitations. The value of the entropy change (ΔS) calculated from the magnetic specific heat is nearly equal to that expected for a $S = 1/2$ system. In the local probe measurements (NMR), we were unable to detect the signal originating from the magnetic vanadium due to the fast on-site fluctuations of the V^{4+} local moments to which the ^{51}V nucleus is strongly coupled and consequently giving rise to very short relaxation times. The ^{51}V signal that was observed by us stems from the nonmagnetic vanadium sites. We found a clear signature of the formation of long-range magnetic order below T_N from the temperature dependent NMR linewidth. Further, we found that the spin-spin relaxation consists of two components. We suggest that the shorter component arises from a coupling through the magnetic regions while the longer one is from non-LRO regions. Below T_N, both nonmagnetic and magnetically ordered regions are found to coexist which, possibly, is characteristic of the inherent frustration in the system. In view of a unique V^{4+} site in the structure, the coexistence might imply the presence of lattice distortions at low temperatures creating inequivalent magnetic environments. Further work using techniques such as muon spin rotation and neutron diffraction is needed to explore this aspect.

ACKNOWLEDGMENTS

Discussions with R. K. Sharma are acknowledged. T.C., A.V.M., A.A.G., and A.V.T. thank the Joint Indo-Russian RFFI-DST Grant No. 11-02-92707- IND for financial support. W.K. and N.B. kindly acknowledge support from the German Research Society (DFG) via TRR80 (Augsburg, Munich).

*mahajan@phy.iitb.ac.in

[1] J. E. Greedan, J. Mater. Chem. **11**, 37 (2001).
[2] R. Moessner and A. P. Ramirez, Phys. Today **59**(2), 24 (2006).
[3] G. Toulouse, Commun. Phys. **2**, 115 (1977).
[4] P. W. Anderson, Science **235**, 1196 (1987).
[5] N. D. Mermin and H. Wagner, Phys. Rev. Lett. **17**, 1133 (1966).
[6] J. G. Bednorz and K. A. Mueller, Z. Phys. B **64**, 189 (1986).
[7] C. K. Majumdar and D. K. Ghosh, J. Math. Phys. **10**, 1399 (1969).
[8] K. Kuboki and H. Fukuyama, J. Phys. Soc. Jpn. **56**, 3126 (1987).
[9] J. M. Law, P. Reuvekamp, R. Glaum, C. Lee, J. Kang, M.-H. Whangbo, and R. K. Kremer, Phys. Rev. B **84**, 014426 (2011).
[10] N. Maeshima, M. Hagiwara, Y. Narumi, K. Kindo, T. C. Kobayashi, and K. Okunishi, J. Phys.: Condens. Matter **15**, 3607 (2003).
[11] H. Kikuchi, H. Nagasawa, Y. Ajiro, T. Asano, and T. Goto, Physica B **284–288**, 1631 (2000).
[12] A. Saul and G. Radtke, Phys. Rev. Lett. **106**, 177203 (2011).
[13] F. Mila, P. Millet, and J. Bonvoisin, Phys. Rev. B **54**, 11925 (1996).
[14] D. C. Johnston, J. W. Johnson, D. P. Goshorn, and A. J. Jacobson, Phys. Rev. B **35**, 219 (1987).
[15] M. A. Korotin, I. S. Elfimov, V. I. Anisimov, M. Troyer, and D. I. Khomskii, Phys. Rev. Lett. **83**, 1387 (1999).
[16] R. E. Marsh, J. Solid State Chem. **122**, 245 (1996).
[17] J. Rodriguez-Carvajal, Physica B **192**, 55 (1993).
[18] T. Chirayil, P. Y. Zavalij, and M. S. Whittingham, Chem. Mater. **10**, 10 (1998).
[19] P. W. Selwood, *Magnetochemistry* (Interscience, New York, 1956).
[20] S. Derakhshan, J. E. Greedan, and L. M. D. Cranswick, Phys. Rev. B **77**, 014408 (2008).
[21] F. Heidrich-Meisner, A. Honecker, and T. Vekua, Phys. Rev. B **74**, 020403(R) (2006). The heat capacity is nearly unaffected by the interchain coupling; A. Honecker (private communication).
[22] For detailed numerical tables see http://www.theorie.physik.uni-goettingen.de/honecker/j1j2-td/.
[23] R. L. Carlin, *Magnetochemistry* (Springer-Verlag, Berlin, 1986).
[24] J. Van Kranendonk and J. H. Van Vleck, Rev. Mod. Phys. **30**, 1 (1958).
[25] M. A. Vachon, W. Kundhikanjana, A. Straub, V. F. Mitrovic, A. P. Reyes, P. Kuhns, R. Coldea, and Z. Tylczynski, New J. Phys. **8**, 222 (2006).
[26] A. Narath, Phys. Rev. **162**, 320 (1967). Note that for a saturating pulse width much smaller than T_1, the formula applicable for the recovery of the longitudinal magnetization for an $I = 7/2$ nucleus when the central line is saturated is $1 - M(t)/M_0 = 0.012e^{(-Wt)} + 0.068e^{(-6Wt)} + 0.206e^{(-15Wt)} + 0.714e^{(-28Wt)}$. This, however, did not fit our data well.